On checking causality of bandlimited sampled frequency responses

On checking causality of bandlimited sampled frequency responses

Piero Triverio, Stefano Grivet-Talocia
Dept. of Electronics, Politecnico di Torino
C. Duca degli Abruzzi 24, 10129 Torino, Italy
Email: piero.triverio@polito.it, grivet@polito.it

***Abstract*— We propose a new technique for checking causality and self-consistency of bandlimited sampled frequency responses. The main algorithm is based on an efficient numerical implementation of the Generalized Hilbert transform. The key advantage of the proposed formulation is the explicit derivation of error bounds for the unavoidable sources of inaccuracy due to the finite number of available frequency samples. These bounds are used for detecting any significative causality violations in the data under analysis. The proposed scheme can be applied in CAD environment to certify the quality of frequency data coming either from measurement or simulation, before using the data in the actual design flow.**

I. Introduction and motivations

The application area for this research activity is the design of high-speed interconnect structures under Signal Integrity constraints. It is widely recognized that dispersion, losses, attenuation, and crosstalk are the most limiting factors for high-speed signal transfer through electrical interconnect links. All these spurious effects must be modeled in early stages of the design flow in order to guarantee signal quality and error-free digital transmission.

Most CAD tools allow system-level simulation for Signal Integrity by computing and connecting together models for the various subparts, such as connectors or via arrays, including all relevant signal degradation effects. These models are usually based on rational approximations of raw frequency responses [1], since this form can be readily incorporated into common circuit solvers (SPICE) via standard techniques. The success of this model derivation depends on the quality of the original frequency responses, which are usually derived either via direct measurement (if possible), or via full-wave electromagnetic simulation. However, frequency-dependent measurement errors in the first case, and errors due to the numerical discretization in the second case, may seriously affect the quality of the frequency characterization. When these errors are large, model derivation becomes difficult and may even fail.

We propose in this paper a technique for certifying the quality of raw frequency responses based on a causality check. In fact, it is well-known that real and imaginary parts of any frequency response representing a causal system are related by Hilbert transform [2] or, equivalently, dispersion relations. These relations have been exploited in several areas of engineering and physics: a comprehensive list of applications and bibliographic references can be found in [3]. Causality violations have been reported to be one of the possible cause for the failure of commonly used macromodeling algorithms [4] and can be detected by means of Hilbert transform [5], [6]. However, the accurate verification of dispersion relations for bandlimited data is still an open problem [3], [7]. We address this issue by introducing a causality verification tool based on an efficient implementation of the Generalized Hilbert transform. Explicit error bounds due to finite frequency resolution and bandwidth are derived and used to unbias the check from systematic errors. We perform a thorough investigation on the resolution of the proposed technique, which is demonstrated to allow detection of very small causality violations.

II. Preliminaries

We consider a physical system described via its input-output behavior

$$y(t) = h(t) * x(t) \quad \Leftrightarrow \quad Y(j\omega) = H(j\omega)X(j\omega)\,, \qquad (1)$$

with $x(t)$, $y(t)$ describing the input and output variables, respectively, and $h(t)$ being the system impulse response. The corresponding frequency-domain representation involves the system transfer function $H(j\omega)$. We will denote with $U(\omega)$ and $V(\omega)$ the real and imaginary parts of $H(j\omega)$ as functions of frequency. Throughout this work we will consider single-input single-output systems. However, there is no loss of generality since the properties that we are going to investigate apply to any entry of the transfer matrix for a generic multiple-input multiple-output system.

Causality is a basic principle stating that any effect must not precede its cause. This causality principle requires the system impulse response to be vanishing for negative times, $h(t) = 0, \ t < 0$. This condition, when expressed in frequency domain, implies that the real and imaginary parts of the transfer function are not independent but are related by Hilbert transform or, equivalently, satisfy the Kramers-Krönig dispersion relations [2]

$$U(\omega) = \frac{1}{\pi} \fint V(\omega') \frac{d\omega'}{\omega - \omega'} \qquad (2a)$$

$$V(\omega) = -\frac{1}{\pi} \fint U(\omega') \frac{d\omega'}{\omega - \omega'} \qquad (2b)$$

where all integrals are defined according to Cauchy principal value. Throughout this paper, unless explicitly noted, any integral extends from $-\infty$ to $+\infty$.

1-4244-0157-7/06/$20.00 ©2006 IEEE

III. Robust causality check

We restate the dispersion relations (2) under a slightly different perspective. We define a reconstruction operator

$$\widehat{H}(j\omega) = \widehat{U}(\omega) + j\widehat{V}(\omega) = \mathcal{R}_0\{H(j\omega)\}, \tag{3}$$

where

$$\widehat{H}(j\omega) = \frac{1}{j\pi}\int H(j\omega')\frac{d\omega'}{\omega-\omega'} \tag{4}$$

is derived by merging (2a) and (2b). Clearly, if $H(j\omega)$ represents a causal system, we have $\widehat{H}(j\omega) = H(j\omega)$, i.e., $\mathcal{R}_0$ is the identity operator. Conversely, when causality violations are present in $H(j\omega)$, the reconstructed $\widehat{H}(j\omega)$ is different, and we can define a reconstruction error as

$$\Delta_0(j\omega) = \widehat{H}(j\omega) - H(j\omega) \tag{5}$$

The strategy that we pursue in this work to test for causality is to compute this consistency error and to check its magnitude against some suitable frequency-dependent threshold. Unfortunately, direct application of (4) generally fails due to the following reasons:

1) The asymptotic behavior of commonly-used system representations may not vanish for $|\omega| \to \infty$. This is the case, e.g., for impedance, admittance, or scattering representations of electrical one-port and multi-ports. This makes the Hilbert transform ill-defined and requires more advanced formulations suitable for numerical implementation.
2) Measurements or simulations lead to sampled data over a limited frequency range. We assume available data as
$$H(j\omega_k), \quad k = -K, \ldots, K \tag{6}$$
with $\omega_{\pm K} = \pm\Omega$ defining the bandwidth (if only positive frequencies are known, basic symmetry conditions for real-valued impulse responses are used to recover the negative part of the spectrum). This prevents the exact application of the reconstruction operator, leading to both a truncation error and a discretization error in the numerically reconstructed data. It is therefore important to estimate these errors in order to design a sound numerical test.

The above points are addressed in the following sections.

A. Generalized dispersion relations

The possibly non-vanishing behavior of $H(j\omega)$ for large frequencies combined with data availability over a limited frequency range is a potentially serious source of inaccuracy for the proposed technique. Therefore, we consider the so-called dispersion relations with subtractions [8] (also denoted as generalized Hilbert transform), which are shown in [4] to significantly improve the numerical performance. First, we identify a set of *subtraction points* $\{\bar{\omega}_q\}_{q=1}^n$ spanning the available bandwidth $[-\Omega, \Omega]$ and we formally derive the Lagrange interpolation polynomial based on these points

$$\mathcal{L}_H(j\omega) = \sum_{q=1}^{n} H(j\bar{\omega}_q) \prod_{\substack{p=1 \\ p\neq q}}^{n} \frac{\omega-\bar{\omega}_p}{\bar{\omega}_q-\bar{\omega}_p} \tag{7}$$

Next, we subtract this polynomial from $H(j\omega)$, and we divide by the n-degree polynomial with roots in the subtraction points before applying the standard Hilbert transform. The resulting expression

$$\widehat{H}(j\omega) = \mathcal{R}_n\{H(j\omega)\} = \mathcal{L}_H(j\omega) + \frac{\prod_{q=1}^n(\omega-\bar{\omega}_q)}{j\pi}\int \frac{H(j\omega')-\mathcal{L}_H(j\omega')}{\prod_{q=1}^n(\omega'-\bar{\omega}_q)}\frac{d\omega'}{\omega-\omega'}$$

defines a generalized reconstruction operator. The corresponding reconstruction error becomes

$$\Delta_n(j\omega) = \mathcal{R}_n\{H(j\omega)\} - H(j\omega)\,. \tag{8}$$

B. Truncation error

We focus now on the numerical evaluation of the reconstruction error (8). First, we extract an error term due to missing information for $|\omega| > \Omega$. We have

$$\Delta_n(j\omega) = \Delta_{\Omega,n}(j\omega) + E_n(j\omega)\,, \tag{9}$$

where

$$\begin{aligned}\Delta_{\Omega,n}(j\omega) &= \mathcal{L}_H(j\omega) - H(j\omega) \\ &+ \frac{\prod_{q=1}^n(\omega-\bar{\omega}_q)}{j\pi}\int_{-\Omega}^{\Omega}\frac{H(j\omega')}{\prod_{q=1}^n(\omega'-\bar{\omega}_q)}\frac{d\omega'}{\omega-\omega'} \\ &- \frac{\prod_{q=1}^n(\omega-\bar{\omega}_q)}{j\pi}\int\frac{\mathcal{L}_H(j\omega')}{\prod_{q=1}^n(\omega'-\bar{\omega}_q)}\frac{d\omega'}{\omega-\omega'}\end{aligned} \tag{10}$$

can be evaluated numerically and the truncation error is defined as

$$E_n(j\omega) = \frac{\prod_{q=1}^n(\omega-\bar{\omega}_q)}{j\pi}\int_{|\omega'|>\Omega}\frac{H(j\omega')}{\prod_{q=1}^n(\omega'-\bar{\omega}_q)}\frac{d\omega'}{\omega-\omega'}$$

The advantage of using the generalized Hilbert transform with several subtraction points is evident from this expression, since the significance of this error term is lowered by the polynomial term in the denominator.

Depending on the behavior of $H(j\omega)$ for high-frequencies, a suitable bound for $E_n(j\omega)$ can be derived: for example, scattering responses of passive circuits are such that $|H(j\omega)| \leq 1$ at any frequency. In this case one can write

$$|E_n(j\omega)| \leq T_n(\omega) \tag{11}$$

where

$$T_n(\omega) = \frac{1}{\pi}\sum_{q=1}^{n}\left[\left|\ln\frac{\Omega-\bar{\omega}_q}{\Omega-\omega}\right| - (-1)^n\left|\ln\frac{\Omega+\bar{\omega}_q}{\Omega+\omega}\right|\right] \times \prod_{\substack{p=1 \\ p\neq q}}^{n}\frac{|\omega-\bar{\omega}_p|}{\bar{\omega}_q-\bar{\omega}_p}$$

Similar bounds can be derived for the impedance and admittance representations. It is straightforward to verify that $|E_n(j\omega)|$ is bounded between any pair of subtraction points by a constant that is decreasing with increasing n. In addition, the bound $T_n(\omega)$ can be further minimized with an appropriate placement of subtraction points $\bar{\omega}_q$, e.g., by a Chebyshev distribution, see [4].

C. Discretization error

Having computed a bound for the contribution of the unknown out-of-band part of the spectrum, we focus now on the evaluation of $\Delta_{\Omega,n}(j\omega)$. Note that the last integral in (10) is known analytically. Conversely, some quadrature rule is required for the numerical computation of the first integral, thus introducing a discretization error $D(j\omega)$. We denote the numerically computed reconstruction error as

$$\widetilde{\Delta}_{\Omega,n}(j\omega) = \Delta_{\Omega,n}(j\omega) + D(j\omega) \tag{12}$$

We remark that, due to the singular nature of the Hilbert kernel, a singularity extraction via

$$\fint_{-\Omega}^{\Omega} g(\omega')\frac{d\omega'}{\omega-\omega'} = \int_{-\Omega}^{\Omega}\frac{g(\omega')-g(\omega)}{\omega-\omega'}d\omega' - g(\omega)\ln\left|\frac{\Omega-\omega}{\Omega+\omega}\right|$$

is performed to regularize the integrals before applying the quadrature rule. Then, an estimate of the discretization error

$$|D(j\omega)| \simeq \widetilde{D}(\omega)$$

is obtained by applying two different quadrature methods with different order and by computing the difference in the results.

D. The causality check

An ideal causality check would test whether the exact reconstruction error $\Delta_n(j\omega)$ is identically vanishing (no causality violations) or not. However, only its numerical estimation $\widetilde{\Delta}_{\Omega,n}(j\omega)$ is known and differs from $\Delta_n(j\omega)$ because of truncation and discretization errors

$$\widetilde{\Delta}_{\Omega,n}(j\omega) = \Delta_n(j\omega) - E_n(j\omega) + D(j\omega)\,. \tag{13}$$

The above estimates for these errors lead to the definition of a rigorous worst-case threshold

$$E_n^{\mathrm{tot}}(\omega) = T_n(\omega) + \widetilde{D}(\omega) \tag{14}$$

to be compared with $\widetilde{\Delta}_{\Omega,n}(j\omega)$. If, at some frequency point ω_l, the estimation of the reconstruction error exceeds this threshold

$$\left|\widetilde{\Delta}_{\Omega,n}(j\omega_l)\right| > E_n^{tot}(\omega_l) \tag{15}$$

we are confident that causality violations are present because, owing to the following inequality

$$|\Delta_n(j\omega_l)| \geq \left|\widetilde{\Delta}_{\Omega,n}(j\omega_l)\right| - |E_n(j\omega_l) - D(j\omega_l)| \gtrsim \left|\widetilde{\Delta}_{\Omega,n}(j\omega_l)\right| - E_n^{tot}(\omega_l)\,,$$

the exact reconstruction error $\Delta_n(j\omega_l)$ is nonvanishing. Conversely, if

$$\left|\widetilde{\Delta}_{\Omega,n}(j\omega_k)\right| \leq E_n^{tot}(\omega_k) \quad \forall k \tag{16}$$

is satisfied at all available frequency points, any causality violation in the data is not distinguishable from the unavoidable errors due to the numerical computation of dispersion relations. In other words, the frequency-dependent threshold (14) gives the "resolution" of the numerical causality verification tool.

IV. Discussion

Here we discuss the performance of the proposed technique in the detection of causality violations of a given frequency response $H(j\omega)$. We assume

$$H(j\omega) = H_c(j\omega) + P(j\omega) = H_c(j\omega) + P_c(j\omega) + P_a(j\omega)$$

where $H_c(j\omega)$ is the true (unknown) and certainly causal system response. The perturbation term $P(j\omega)$ may represent measurement or simulation errors, which are further decomposed into a causal part $P_c(j\omega)$ and an anti-causal part $P_a(j\omega)$, i.e., having inverse Fourier transform $p_a(t)$ vanishing for $t > 0$. We remark that modified dispersion relations hold also for anti-causal responses, in this case

$$P_a(j\omega) = \mathcal{L}_{P_a}(j\omega) - \frac{\prod_{q=1}^{n}(\omega-\bar{\omega}_q)}{j\pi}\int\frac{P_a(j\omega')-\mathcal{L}_{P_a}(j\omega')}{\prod_{q=1}^{n}(\omega'-\bar{\omega}_q)}\frac{d\omega'}{\omega-\omega'}\,. \tag{17}$$

Taking into account that both causal terms $H_c(j\omega)$ and $P_c(j\omega)$ do not contribute to the reconstruction error $\Delta_n(j\omega)$, we have the following expression for its numerical estimation (13)

$$\widetilde{\Delta}_{\Omega,n}(j\omega) = \mathcal{L}_{P_a}(j\omega) - P_a(j\omega) - E_n(j\omega) + D(j\omega) + \frac{\prod_{q=1}^{n}(\omega-\bar{\omega}_q)}{j\pi}\int\frac{P_a(j\omega')-\mathcal{L}_{P_a}(j\omega')}{\prod_{q=1}^{n}(\omega'-\bar{\omega}_q)}\frac{d\omega'}{\omega-\omega'}\,. \tag{18}$$

Combining now (18) with (17), we obtain

$$\widetilde{\Delta}_{\Omega,n}(j\omega) = 2[\mathcal{L}_{P_a}(j\omega) - P_a(j\omega)] - E_n(j\omega) + D(j\omega)\,. \tag{19}$$

This implies

$$|\widetilde{\Delta}_{\Omega,n}(j\omega_l)| \geq 2\,|P_a(j\omega_l) - \mathcal{L}_{P_a}(j\omega_l)| - |E_n(j\omega_l) - D(j\omega_l)| \gtrsim 2\,|P_a(j\omega_l) - \mathcal{L}_{P_a}(j\omega_l)| - E_n^{tot}(\omega_l)\,.$$

Therefore, the proposed test condition (15) is certainly satisfied (the causality violation is detected by the numerical test) when

$$|P_a(j\omega_l) - \mathcal{L}_{P_a}(j\omega_l)| > E_n^{tot}(\omega_l)\,. \tag{20}$$

In summary, a causality violation is detectable when it remains sufficiently large after extraction of its Lagrange polynomial.

We conclude this section by discussing the influence of the number n of subtraction points. In general, the resolution of the causality check increases with n, because the truncation error decreases. Only when $|P_a(j\omega) - \mathcal{L}_{P_a}(j\omega)|$ decreases faster than $T_n(\omega)$ for all frequencies, a large number of subtractions is not useful. This particular situation occurs only for very smooth causality violations, in which case the Lagrange polynomial $\mathcal{L}_{P_a}(j\omega)$ converges quickly to $P_a(j\omega)$ as n grows. Noting that all polynomials satisfy the causality conditions (at least in distributional sense), we conclude that any smooth causality violation is "very close" to causal, henceforth intrinsically difficult to be detected by any numerical test. In all other situations when $P_a(j\omega)$ is not everywhere smooth (e.g., when data are affected by measurement noise), the proposed method is able to detect very weak causality violations as n grows.

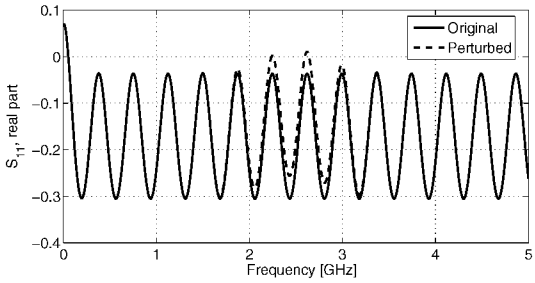

Fig. 1. Original and perturbed return loss S_{11}.

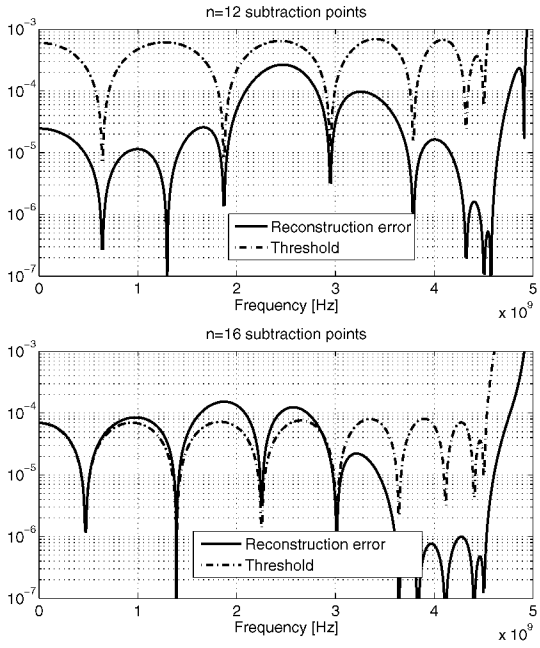

Fig. 2. Comparison of numerically evaluated reconstruction error (solid line) and frequency-dependent threshold (dashed line) with $n = 12$ (top) and $n = 16$ (bottom) subtraction points, for a perturbation amount $A = 5 \times 10^{-4}$.

V. Numerical examples

In this section we systematically investigate the resolution of the proposed method on a simple test case. We computed the scattering responses of a 10-cm transmission line having per-unit-length parameters $L = 4.73\,\mathrm{nH/cm}$, $C = 3.8\,\mathrm{pF/cm}$, $R = 0.8\,\Omega/\mathrm{cm}$, $G = 0$. Then, we perturbed only the real part of S_{11} by adding a smooth gaussian-shaped term $\Gamma(\omega) = A\exp\{-\alpha(\omega-\omega_0)^2\}$ centered at 2.5 GHz and with bandwidth 1 GHz. The perturbation amplitude is varied to investigate the performance of the causality test. Figure 1 shows the raw and perturbed responses for a large amount of perturbation $A = 5 \times 10^{-2}$, to make it visible in the plot. Figure 2 reports the computed reconstruction error $\widetilde{\Delta}_{\Omega,n}(j\omega)$ and compares it to the threshold $E_n^{tot}(\omega)$ for two different sets of subtraction points. In these plots, a very small amplitude $A = 5 \times 10^{-4}$ (i.e., 100 times smaller than in Fig. 1) is used to make the violation hard to detect. In top panel we used $n = 12$, with a corresponding estimate for the truncation error $T_n \sim 7 \times 10^{-4}$. In bottom panel, we used $n = 16$, corresponding to $T_n \sim 8 \times 10^{-5}$. The violation is detected only using a large n, since a very fine resolution is required.

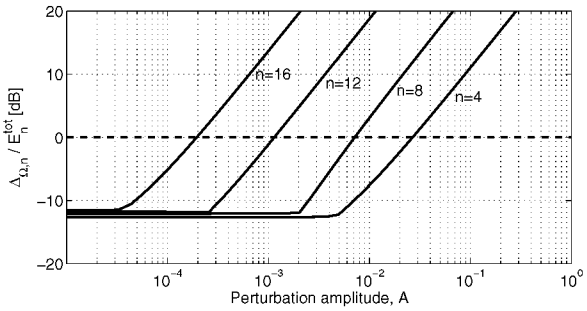

Fig. 3. Normalized reconstruction error as a function of perturbation amplitude A.

Finally, we ran a sweep on the amplitude A to illustrate the algorithm sensitivity. The results are depicted in Fig. 3, where the maximum (over frequency) computed reconstruction error is normalized to the threshold and plotted for $n = 4, 8, 12, 16$ subtraction points. Successful detection occurs when the resulting numerical estimate is larger than the 0 dB baseline. This plot illustrates the increased resolution for increased n, and the capability of detecting even very small violations by tuning the number of subtraction points.

VI. Conclusions

We have introduced a numerical tool based on a special formulation of the generalized Hilbert transform for the detection of causality violations in sampled bandlimited frequency responses. The numerical implementation of the test is based on formally derived error bounds which allow to predict the effective resolution of the algorithm. In addition, this resolution can be tuned by choosing an appropriate number of so-called subtraction points. As a result, we have obtained a highly reliable and robust algorithm, which is immediately applicable for the certification of the self-consistency of frequency responses before they are extensively used in a CAD environment for system-level analysis and design purposes.

References

[1] B. Gustavsen and A. Semlyen, "Rational approximation of frequency domain responses by Vector Fitting," *IEEE Trans. Power Delivery*, vol. 14, no. 3, pp. 1052–1061, July 1999.

[2] S. L. Hahn, "Hilbert transforms," in *The Transforms and Applications Handbook*, A. D. Poularikas, Ed. CRC and IEEE, 2000.

[3] K. R. Waters, J. Mobley, J. G. Miller, "Causality-Imposed (Kramers-Krönig) Relationships Between Attenuation and Dispersion," *IEEE Trans. Ultrason., Ferroelect., Freq. Contr.*, vol. 52, pp. 822–833, 2005.

[4] P. Triverio and S. Grivet-Talocia, "A robust causality verification tool for tabulated frequency data," in *10th IEEE Workshop on Signal Propagation on Interconnects, Berlin, Germany*, May 9–12, 2006 (submitted).

[5] J. R. James, G. Andrasic, "Assessing the accuracy of wideband electrical data using Hilbert transforms," *IEE Proc.*, vol. 137, pp. 184–188, 1990.

[6] F. M. Tesche, "On the Use of the Hilbert Transform for Processing Measured CW Data," *IEEE Trans. Electromagn. Compat.*, vol. 34, pp. 259–266, 1992.

[7] G. W. Milton, D. J. Eyre, J. V. Mantese, "Finite Frequency Range Kramers Kronig Relations: Bounds on the Dispersion," *Phys. Rev. Lett.*, vol. 79, pp. 3062–3065, 1997.

[8] N. M. Nussenzveig, *Causality and dispersion relations*. Academic Press, 1972.